Controlled Synthesis of Nanoscale Icosahedral Gold Particles at Room Temperature

12 AUTHORS, INCLUDING:

Juncheng Hu
South-Central University For Nationalities
67 PUBLICATIONS **1,289** CITATIONS

Sergey V. Prikhodko
University of California, Los Angeles
72 PUBLICATIONS **481** CITATIONS

Marta Pozuelo
University of California, Los Angeles
48 PUBLICATIONS **410** CITATIONS

Ryan M Richards
Colorado School of Mines; National Renew…
133 PUBLICATIONS **2,541** CITATIONS

Controlled Synthesis of Nanoscale Icosahedral Gold Particles at Room Temperature

Lifang Chen,[a, c] G. Jeremy Leong,[a, b] Maxwell Schulze,[a] Huyen N. Dinh,[b] Bryan Pivovar,[b] Juncheng Hu,[d] Zhiwen Qi,*[c] Yunjin Fang,[c] Sergey Prikhodko,[e] Marta Pozuelo,[e] Suneel Kodambaka,[e] and Ryan M. Richards*[a]

The shape of nanocrystals determines surface atomic arrangement and coordination, influencing their chemical and physical properties. We present a novel and facile approach to synthesize gold icosahedra by employing glucose as reducing reagent and sodium dodecyl sulfate as directing agent in the environmentally benign medium of water at room temperature. The size of the icosahedra can be controlled in the range of 30–250 nm by altering reaction conditions. High-resolution microscopy and diffraction studies indicate the icosahedra are composed of rotational twins that owe likely to assemblage of tetrahedral units. The gold icosahedra particles catalytic properties are probed in the borohydride reduction of *p*-nitrophenols and exhibit a size-dependence reaction property. Comparison studies with spherical particles prepared by the Turkevich method, coupled with poisoning experiments, infer that the shape has a strong influence in the abundance of active surface sites as well as their activities. The properties of nanoscale icosahedra particles has promising applications for further catalytic processes, surface enhancement spectroscopic methods, chemical or biological sensing, and the fabrication of nanoscale devices.

Introduction

Metal nanostructures have been the focus of intensive research because of their unique size- and shape-dependent chemical and physical properties.[1, 2] In recent years, catalysis by gold particles has become one of the most studied new topics in chemistry.[3] Gold-based catalysts have demonstrated very promising activity and selectivity in many chemical reactions and the catalytic properties have been found to strongly depend on the particle shape, size and environment.[4, 5] Many researchers have focused on rational ways to control the shape and size of gold particles. Many efforts have been made in past decades, to synthesize size- and shape-controlled[6–8] nanostructured metals including rods,[9, 10] plates,[11] spheres[12] and cages.[13] There are some reports on the fabrication of gold crystals with cubic, octahedral, decahedral, dodecahedral and icosahedral morphologies, which are highly faceted, with sharp corners and edges, as well as multiply twinned gold crystals.[14–20] The shape of nanocrystals determines surface atomic arrangement and coordination, further influencing their catalytic performance.[21, 22] To date, the reported gold crystals with the highest proportion of corners and edges are icosahedra and a few papers have been published on these gold systems. Icosahedral gold particles of 230 nm diameter were prepared using ethylene glycol at 280 °C in the presence of poly(vinyl pyrrolidone) (PVP) as a directing agent.[16] A similar method was used to produce icosahedral gold particles of approximately 400 nm at 120 °C in ethylene glycol with the presence of PVP under hydrothermal conditions[23] and particles of approximately 220 nm at 100 °C in the presence of PVP with a thermal process.[24] Size tunable icosahedral gold particles ranging from 10 to 90 nm were produced by a seed-mediated

growth approach[25] and 100 nm–1 μm tunable particles were obtained if growing particles in the presence of triblock copolymers of poly(ethylene oxide)–poly(propylene oxide)–poly(ethylene oxide).[26] These gold particles may have some different physical and chemical properties to those of un-twinned nanoparticles without sharp corners because of their intrinsic structural characteristics concerning surface energy and lattice

[a] Dr. L. Chen,+ G. J. Leong,+ M. Schulze, Prof. R. M. Richards
Department of Chemistry and Geochemistry
Colorado School of Mines
Golden, CO, 80401 (USA)
Fax: (+ 1) 303-2733629
E-mail: rrichard@mines.edu

[b] G. J. Leong,+ Dr. H. N. Dinh, Dr. B. Pivovar
Hydrogen Systems and Technologies Center
National Renewable Energy Laboratory
Golden, CO, 80401 (USA)

[c] Dr. L. Chen,+ Prof. Z. Qi, Y. Fang
State Key Laboratory of Chemical Engineering
East China University of Science and Technology
Shanghai, 20023 (P.R. China)

[d] Prof. J. Hu
Key Laboratory of Catalysis and Materials Science
of the State Ethnic Affairs Commission &
Ministry of Education South-Central University for Nationalities
Wuhan, 430074 (P.R. China)

[e] Dr. S. Prikhodko, Dr. M. Pozuelo, Prof. S. Kodambaka
Department of Materials Science and Engineering
University of California
Los Angeles, CA 90024 (USA)

[+] These two authors contributed equally to this work.

Supporting information for this article is available on the WWW under http://dx.doi.org/10.1002/cctc.201200230.

Table 1. Summary of icosahedral gold literature.

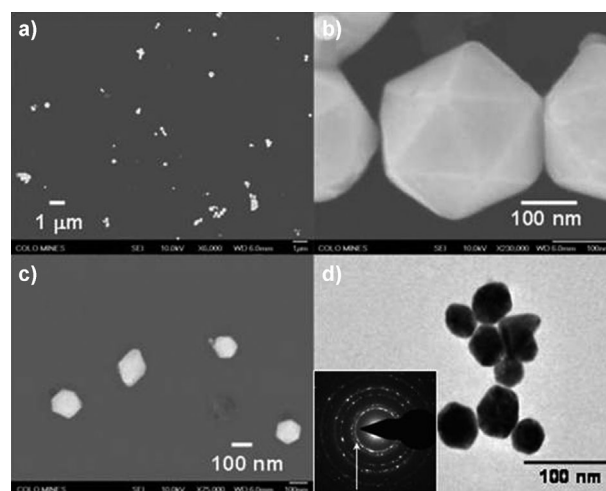| Authors	Size [nm]	Yield [%]
Chen and co-workers[24]	180–250	<80
Yang and co-workers[16]	230	>90
Han and co-workers[25]	11–87 (highly tunable)	>95
Zhang and co-workers[23]	160	80
Murphy and co-workers[27]	100 (tunable shapes)	90
Han and co-workers[26]	100–1000	70
Geng and co-workers[28]	45–50	90

Figure 1. a, b) Field emission scanning electron microscopy (FESEM) images of the Au-250 at different magnifications. c) FESEM image of the Au-100. d) TEM image of the Au-30; inset shows the SAED pattern of the entire image.

symmetry. The previously reported synthesis methods for icosahedral Au are summarized in Table 1.

The development of versatile, simple, and greener methods to prepare gold nanostructures with strongly facetted surfaces and atomically abrupt edges remains a challenging topic. Herein, we present a novel and facile approach to synthesize 30–250 nm gold icosahedra by employing glucose as the reducing reagent and sodium dodecyl sulfate (SDS) as the directing agent in the environmentally benign medium of water at room temperature. This method fully adopts the fundamental principles of "green" chemistry.[29] Moreover, the sizes of the obtained gold icosahedra can be tuned and these gold icosahedron nanoparticles showed high activity in the reduction of *p*-nitrophenol by sodium borohydride. Additionally, comparison studies with spherical particles and poisoning experiments demonstrate the importance of shape on the catalytic properties.

Results and Discussion

Morphology and crystallinity

The gold icosahedra nanostructures, with different sizes prepared at room temperature with a reaction time of 48 h, were analyzed using field emission scanning electron microscopy (FESEM) and TEM, as shown in Figure 1. The labels Au-250, Au-100, and Au-30 in Figure 1 and in the following sections correspond to particles with average diameters of 250, 100, and 30 nm, respectively. The sizes of the gold icosahedra were controlled by varying the initial concentration of $HAuCl_4$ in the solution.

The sizes of gold icosahedra increased as the initial concentration of $HAuCl_4$ was increased, as shown in Table 2. If the initial concentration of $HAuCl_4$ was 0.06235 mm (entry 1), no precipitate was observed, even after stirring for more than seven days. The solution maintained a clear color until a color change was observed shortly before 48 h. The observed trends in color for this gold system were indicative of slow growth rates, which owed likely to the weak reduction potential of glucose. The color of the solution remained pink and there was no further growth over 48 h. Smaller Au nanoparticles do not grow continuously, owing to low concentrations of $HAuCl_4$, and there was no additional supply of gold atoms from continued precursor decomposition.[1] With increased $HAuCl_4$ concentration, icosahedra-like Au particles started to form (see Table S2, entry 2 in the Supporting Information). If initial $HAuCl_4$ concentration continued to increase, gold icosahedra nanoparticles formed (Table 2, entries 3–5). However, irregular Au nanoparticles formed if the $HAuCl_4$ concentration was 2.275 mm. A large amount of precipitate formed in a few minutes owing to the higher $HAuCl_4$ concentration, which resulted in fast nucleation and growth. Moreover, the color of the solution was transparent and indicated that all of the $HAuCl_4$ was reduced to Au nanoparticles in a very fast reduction process. In Figure 1a, the sample was observed to contain numerous particles with sizes of approximately 250 nm. The higher magnification FESEM image (Figure 1b) clearly revealed the 3D shape of the icosahedral gold particles with a size of (250 ± 40) nm. Detailed structural characterization of the particles was performed using TEM and selected area electron diffraction (SAED) pattern. Figure 1d is a representative bright-field TEM image. We found that the as-synthesized samples contained nanoparticles with several different polyhedral shapes of which the majority (>60%) were icosahedra (from TEM). Some irregularly shaped particles were also observed, which were by-products of the reaction. A typical SAED pattern acquired from the sample is shown as an inset in Figure 1d. By indexing the diffraction pattern, we identified the structure as face centered cubic (fcc) gold space group: *Fm3m*, (2 2 5), JCPDS No. 040784. Measured interplanar spacings coincided with JCPDS values

Table 2. Correlation between Au concentration and particle size.

Entry	Concentration [mm $HAuCl_4$]	Aliquot [µL]	Size [nm]	Shape
1	0.0623	50	2–5	dots
2	0.124	100	20	pentagonal
3	0.3086	250	30	icosahedral
4	0.610	500	100	icosahedral
5	1.19	1000	250	icosahedral
6	2.27	2000	500	irregular particles

(see Table S1), indicating that the powders were phase-pure and crystalline Au.

Figure 2a is a typical high-resolution (HR)TEM image of an individual gold icosahedron with a diameter of 30 nm. From the lattice fringes seen in the image, we measured the interplanar spacings of 0.21 and 0.24 nm, which corresponded to {200} and {111} planes in gold, respectively. Arrows highlight the Moiré fringes, which appear to result from overlapping of multiple crystals. Note the presence of twin defects at the intersection of facets. All of these structural features were observed in all the examined nanoparticles. Figure 2b is an SAED pattern of the particle shown in Figure 2a. From the indexing of the diffraction pattern, we found 6 {111} spots, labeled 1–6 in Figure 2b. This could only be explained by the presence of multiple crystals and is discussed in detail below. The other spots labeled 7–9 represent {200}, 10–14 to {220}, and 15–21 to {222}/{311}.

From the analyses of the diffraction pattern, we found that the nanoparticle was composed of multiple fcc Au crystallites. This is illustrated in Figure 2c using a schematic of the color-coded reciprocal lattice. This is illustrated in Figure 2c using a schematic of the color coded reciprocal lattice. Sizes of the reciprocal spots in Figure 2c are representative to tabulated (JCPDS) intensities. The green color spots denote reciprocal lattice points that result from crystallites, all of which share the [111] zone axis and are rotated by 60° with respect to each other. These rotational variants, that is, twins, can be represented by the orientation relationship [Eq. (1)]:

$$\{111\}o \parallel \{111\}t, \ <011>o \parallel <011>t \tag{1}$$

in which the subscripts o and t represent orientations of the original and twin crystals, respectively. The red, purple, and blue colors denote three twins all of which share the same [112] zone axis and are rotated by 60° with respect to each other. Those rotational twins can be described by a different orientation relationship [Eq. (2)]:
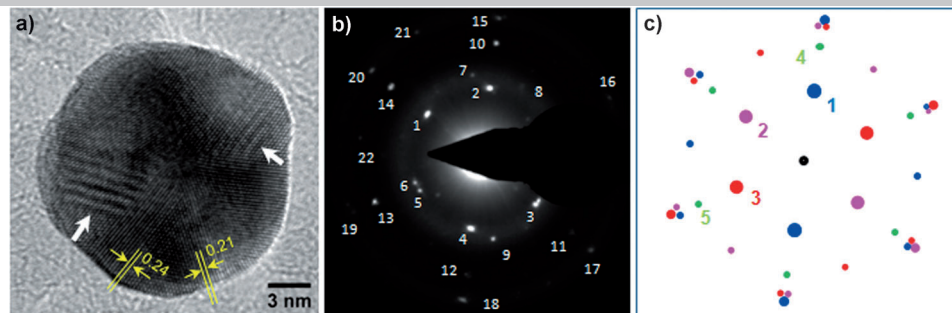

Figure 2. a) HRTEM image of an Au icosahedron. Arrows highlight Moiré patterns observed in the particle. b) SAED pattern of the particle. c) Reconstruction of the reciprocal lattice of multiply twinned icosahedron nanoparticle.
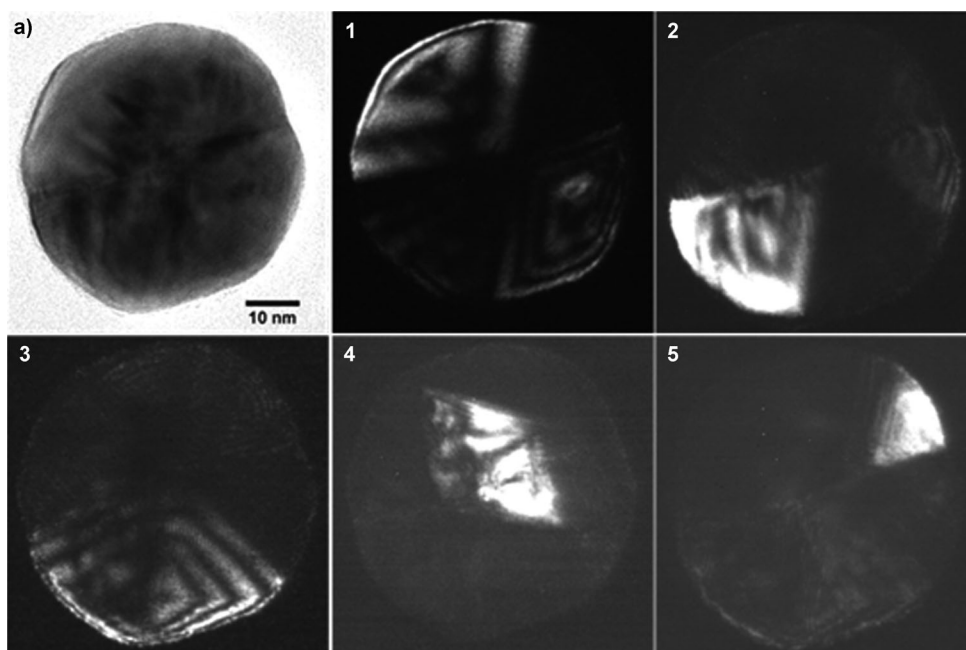

Figure 3. a) HRTEM image of the Au-30 particle with icosahedron shape. 1–5 are dark-field TEM images of the same particle. Images 1, 2, and 3 are obtained from the {111} diffraction spots labeled 1–3 in Figure 2c, and images 4 and 5 are obtained from the {220} spots 4 and 5.

$$\{111\}o \parallel \{112\}t, \ <011>o \parallel <111>t \tag{2}$$

The multiply twinned structure of the Au nanoparticles was confirmed by using TEM in the dark-field mode. Figure 3a is a bright-field TEM image of an individual Au nanoparticle. Figures 3.1–3.5 are dark-field TEM images obtained using the diffraction spots 1–5 labeled in the SAED pattern. The brighter contrast within each of these images is a result of diffraction from one or more crystallites that are aligned to satisfy Bragg's conditions. The triangular shape of the brighter contrast in images 2 and 5 can be interpreted as the 2D projection of a tetrahedral crystal. The diamond-shaped contrasts in images 1, 3, and 4 are the 2D projections of tetrahedral crystallites within the icosahedron suggesting the presence of twinning between the two adjacent tetrahedral crystallites. Multiply twinned Au icosahedra were previously observed and the exis-

tence of twins is attributed to the arrangement of smaller tetrahedral units with {111} facets so that all 20 facets of icosahedron are {111} planes.[30,31] Periodically alternating darker and lighter grey contrast bands observed in the images 1 and 3 are a result of the thickness variations in 3D crystallites. Non-periodic fringe contrast observed, for example, in images 2 and 4 appear as a result of strain in the crystallites.[30] The above results demonstrate that icosahedral gold nanoparticles can be obtained under a wide range of experimental conditions. However, it is challenging to provide a convincing formation mechanism for the icosahedral gold particles at present. In previous literature, most theories about the role of organic compounds imply that the organic compounds act as simple physical compartments or to control nucleation or to terminate crystal growth by surface poisoning through selective adsorption on certain planes.[30–35] In this case, the large amount of SDS adsorbed on specific crystalline surfaces of gold could significantly decrease their growth rates and lead to a high anisotropic growth and ultimately to the final nanoparticles with icosahedral shape. The results discussed above indicate that the size of the icosahedral particles prepared in this work can be controlled in the range of 30 to 250 nm, suggesting that the icosahedral gold particles were formed at an early stage in the reaction.

Catalytic reduction of *p*-nitrophenol

To ascertain if these particles possess catalytic activity, the icosahedral gold particles were employed for the catalytic reduction of *p*-nitrophenol by $NaBH_4$. This reaction is simple and rapid in the presence of metallic surfaces, which allows us to study whether size effects this system.[37–41] The mixture of *p*-nitrophenol and $NaBH_4$ did not occur in the absence of a catalyst, even after a period of two days, as reported elsewhere.[37–41] However, the addition of a small amount of icosahedral Au particles to the above mixture (Figure 4a and Table 3) caused

Figure 4. a) Successive UV/Vis absorption spectra of the borohydride reduction of *p*-nitrophenol catalyzed by the Au-30 sample. b) Plots of ln A versus time for the reduction of *p*-nitrophenol catalyzed by different gold icosahedron samples: 0.0167 mmol of Au-30 (■), 0.0167 mmol of Au-100 (●), 0.0279 mmol of Au-250 (▲).

Table 3. Catalytic data for borohydride reduction of *p*-nitrophenol by different Au icosahedron samples.

Sample	Au used [mmol]	K_{rc} [s^{-1}]	K_{nor} [mmol^{-1} s^{-1}]
Au-30	0.0167	3.1×10^{-3}	0.186
Au-100	0.0212	1.1×10^{-3}	0.052
Au-250	0.0279	6.6×10^{-4}	0.024
Au spheres[a]	0.0167	1.7×10^{-5}	0.001

[a] Prepared with tri-sodium citrate as reducing agent in $HAuCl_4$ solution.

fading and ultimate bleaching of the yellow color of the reaction mixture in quick succession. Figure 4a shows a typical time-dependent UV/Vis absorption change of the reaction mixture by the addition of the icosahedral gold particles with a diameter of 30 nm. In these spectra, the absorption of *p*-nitrophenol at 400 nm decreased with a concomitant increase of the 300 nm peak of *p*-aminophenol within 25 min after the catalyst addition.[40,41] Similar spectral changes of *p*-nitrophenol
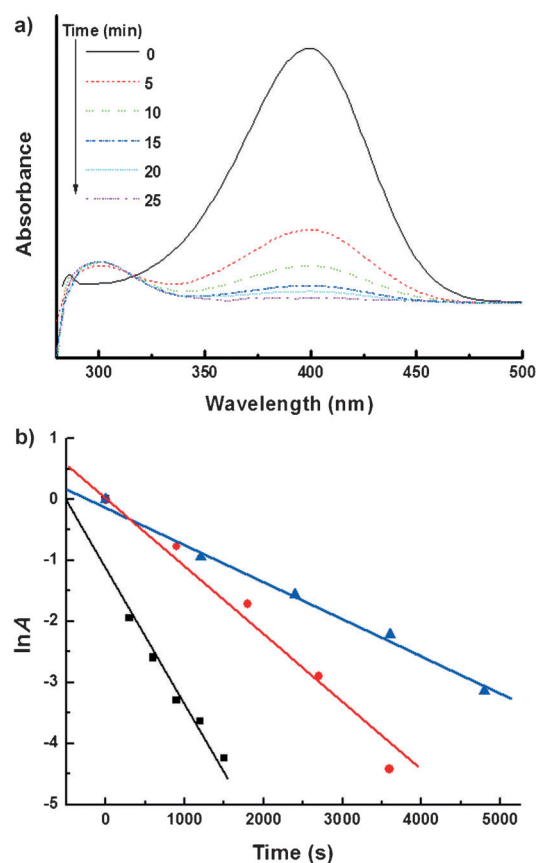
during its reduction were also observed with other icosahedral Au particles, including those of 100 and 250 nm in size in Figures S1 and S2. These results indicated that icosahedral Au particles are able to successfully catalyze the reduction reaction.[41] In this reduction process, as the concentration of $NaBH_4$ in the reaction mixture far exceeded the concentration of *p*-nitrophenol, the $NaBH_4$ concentration remained essentially constant throughout the reaction. The UV/Vis spectra also exhibited an isobathic point between two absorption bands indicating that only two principal species, *p*-nitrophenol and *p*-aminophenol influenced the reaction kinetics. Therefore, pseudo first-order kinetics could be applied for the evaluation of rate constants. The ratio A is of the *p*-nitrophenol absorbencies at time t and at the start, A_t and A_0, respectively. The A_t and A_0 were measured from the relative absorbance values at 400 nm of *p*-nitrophenolate ion. The linear relations of ln A versus time were observed for all catalyst particles, indicating that the reactions followed pseudo first-order kinetics. The rate constants were estimated from diffusion-coupled first-order reaction kinetics using the slopes of straight lines in Figure 4b and shown in Table 3. The rate constants varied from 0.0031 s^{-1} to 0.00066 s^{-1} as the gold icosahedron diameters increased from 30 to 250 nm. We found that the rate constants (k_{rc}) of differ-

ent gold icosahedron particles catalyzed borohydride reduction of *p*-nitrophenol were different with different amount of gold samples. Thus, for coherent comparison, the catalytic activity of different gold icosahedra are presented in terms of the normalized rate constants (k_{nor}), which are obtained by normalizing the k_{rc} values with respect to the total amount (mmol) of catalysts used (see Table 3). Interestingly, the k_{nor} value for sample Au-30 was almost 8 times higher in magnitude than that obtained for Au-250 and was 180 times higher than that of Au spheres prepared by Turkevich method.[42, 43] It was reported that a decrease of the particle size led to an increase in the fraction of low coordination metal sites such as vertices, edges, and surface area, which could promote adsorption of the reactants and facilitate the reaction. This was observed for small particles of less than 5 nm diameter,[44] but our catalysts, in the range of >20 nm, did not show a significant increase of active surface atom fractions. Instead, we believe that the high activity of small particles originated from their large surface area and surface roughness, as observed in the TEM images (Figures 1 d, 2, and 3). The stepwise etching of the metal surface increased surface roughness, generated more defect sites on the surface, and increased the reaction rate.

Quantification of catalytically active sites by CS_2 poisoning

Quantitatively determining the number of active sites is a reliable comparison of catalyst activity and was pursued here to provide insight regarding the role of shape on the catalytic properties. Following a CS_2 poisoning method reported by Finke and co-workers,[45] the catalytic reduction of *p*-nitrophenol was used to probe the number of active sites on icosahedral gold and was compared with that of colloidal gold prepared by the Turkevich method.[42] Multiple gold-catalyzed reduction experiments were performed, each with varying amounts of CS_2 having been added beforehand. By relating the relative amounts of CS_2 added to the relative reaction rate (see Figure S3 and S4), the minimal amount of CS_2 to completely poison and terminate all catalytic activity could be determined for a sample. In the control experiments reported by Finke and co-workers it was demonstrated that the presence of ligand stabilizers reduces the rate of catalytic activity but may not affect the number of active sites able to be poisoned on a catalyst.[45, 46] However, variation of the CS_2 to metal atom ratio can occur between systems depending on reaction conditions such as presence of ligand stabilizers, temperature, and pressure. Therefore, the quantification of active sites by poisoning does not absolutely identify the location or quantity of active sites and is viable only as a comparative approach for this system.[45] The amount of CS_2 required to completely poison a sample was normalized to the amount of gold in the sample (as determined by ICP). It was found that the ratio of CS_2 to completely poison the 40 nm icosahedral gold relative to the 15 nm gold spheres (see Figure S5) prepared by the Turkevich method was approximately 27. Therefore, it is shown quantitatively that the gold icosahedra have nearly 30 times more active sites per mole gold than spherical gold nanoparticles, and each active site is between five and six times more

active on icosahedral gold than spherical gold, as evidenced by the rate constants in Table 3. Notably, the spherical particles are much smaller in diameter and the comparison is thus greatly in favor of the spherical system. The higher activity of icosahedral nanoparticles infers that the growth of {111} facets promoted by SDS produces a more active catalytic sites on icosahedral gold than on spherical gold. Notably, investigations of stabilizer effects on poisoning to clarify poison to metal ratios are ongoing.

Conclusions

We have demonstrated experimentally the direct synthesis of icosahedral gold particles with well-defined shape and tunable sizes (30–250 nm) by a "green" process at room temperature. The icosahedra have been characterized by high-resolution microscopy and electron diffraction that demonstrated they are composed of rotational twins that are probably attributable to the assemblage of tetrahedral units. The gold icosahedron particles were probed for catalytic properties in the borohydride reduction of *p*-nitrophenols, which exhibited a size-dependent reaction property. The catalytic properties of nanoscale icosahedron particles have been examined by poisoning studies that have revealed that as compared to spherical particles prepared by the Turkevich method, the icosahedra have a 30 fold increase in the number of active sites per mole of gold. Furthermore, these sites demonstrate activities 5 fold higher than the spherical particles. This study strongly infers the influence of shape on the abundance and strength of catalytic sites.

Experimental Section

In a typical procedure, the starting solution was prepared by adding glucose (0.63 g) to water (20 mL). SDS (0.65 g) was then added to the aqueous solution under stirring, resulting in a white solution. After the SDS had completely dissolved, HAuCl$_4$·3H$_2$O (25 mM, 0.2–1.0 mL) was added to the solution. After the reaction proceeded for the desired time under continuous stirring, the sample was centrifuged and collected, and washed with distilled water and ethanol several times. Prior to examination and study, the sample was immersed in 0.5 M NaBH$_4$ solution in 1:1 H$_2$O/EtOH for 10 min, then rinsed with ethanol and water. The catalytic reduction reaction was performed in a standard quartz cell with a 1 cm path length and 3 mL volume. The reaction procedures were as follows: A reaction mixture of water (2.8 mL), *p*-nitrophenol (0.1 mL of a 3.0×10^{-1} M solution in water), and NaBH$_4$ (0.1 mL of a 3.0×10^{-1} M solution in water) were combined in the quartz cell. Immediately after addition of purified and dried Au nanoparticles (0.0167 or 0.0279 mmol of sample), the absorption spectra were recorded by a Varian-Cary 300 Scan UV/Vis spectrophotometer with a scanning range of 280–500 nm at 25 °C. Colloidal gold spheres prepared by the Turkevich synthesis were produced as follows. A volume of 1.015 mL HAuCl$_4$·3H$_2$O (25 mM) was added to of refluxing water (94 mL) in a 250 mL round-bottom flask, followed by 1% sodium citrate solution (5 mL), and the solution was stirred at reflux for 15 min. The solution was cooled, centrifuged, and the sample collected and dispersed in ethanol. For the CS_2 poisoning experiments, the above catalytic reduction procedure was used with the addition of varying amounts of 1×10^{-4} to 1×10^{-6} M aqueous CS_2 (0.01–0.3 mL), keeping the total volume of the cell at

2.8 mL. Notably, fresh CS$_2$ solutions needed to be prepared every few hours to obtain consistent results. For concentration determination of the gold nanoparticle samples, aliquots were dried and digested in aqua regia. Concentrations of gold in the samples were found using a PerkinElmer Optima 5300 DV inductively coupled plasma optical emission spectrometer.

Acknowledgements

[1] Y. Xia, Y. Xiong, B. Lim, S. E. Skrabalak, *Angew. Chem.* **2008**, *120*, 8774; *Angew. Chem. Int. Ed.* **2008**, *47*, 8646.

[2] C. Burda, X. Chen, R. Narayanan, M. A. El-Sayed, *Chem. Rev.* **2005**, *105*, 1025.

[3] A. S. K. Hashmi, G. J. Hutchings, *Angew. Chem.* **2006**, *118*, 8064; *Angew. Chem. Int. Ed.* **2006**, *45*, 7896.

[4] W. C. Ketchie, Y. L. Fang, M. S. Wong, M. Murayama, R. J. Davis, *J. Catal.* **2007**, *250*, 94.

[5] L. Chen, J. Hu, R. Richards, *J. Am. Chem. Soc.* **2009**, *131*, 914.

[6] S. Stoeva, K. J. Klabunde, C. M. Sorensen, I. Dragieva, *J. Am. Chem. Soc.* **2002**, *124*, 2305.

[7] M. E. Grass, Y. Yue, S. E. Habas, R. M. Rioux, C. I. Teall, P. Yang, G. A. Somorjai, *J. Phys. Chem. C* **2008**, *112*, 4797.

[8] A. Jakhmola, R. Bhandari, D. B. Pacardo, M. R. Knecht, *J. Mater. Chem.* **2010**, *20*, 1522.

[9] H. A. Keul, M. Moller, M. R. Bockstaller, *Langmuir* **2007**, *23*, 10307.

[10] Y. Niidome, K. Honda, K. Higashimoto, H. Kawazumi, S. Yamada, N. Nakashima, Y. Sasaki, Y. Ishida, J. Kikuchi, *Chem. Commun.* **2007**, 3777.

[11] J. P. Xie, J. Y. Lee, D. I. C. Wang, *J. Phys. Chem. C* **2007**, *111*, 10226.

[12] H. P. Liang, L. J. Wan, C. L. Bai, L. Jiang, *J. Phys. Chem. B* **2005**, *109*, 7795.

[13] J. Y. Chen, B. Wiley, Z. Y. Li, D. Campbell, F. Saeki, H. Cang, L. Au, J. Lee, X. D. Li, Y. N. Xia, *Adv. Mater.* **2005**, *17*, 2255.

[14] D. Seo, J. C. Park, H. Song, *J. Am. Chem. Soc.* **2006**, *128*, 14863.

[15] Y. G. Sun, Y. N. Xia, *Science* **2002**, *298*, 2176.

[16] F. Kim, S. Connor, H. Song, T. Kuykendall, P. D. Yang, *Angew. Chem.* **2004**, *116*, 3759; *Angew. Chem. Int. Ed.* **2004**, *43*, 3673.

[17] J. Zhang, M. R. Langille, M. L. Personick, K. Zhang, S. Li, C. A. Mirkin, *J. Am. Chem. Soc.* **2010**, *132*, 14012.

[18] Y. Chen, X. Gu, C. G. Nie, Z. Y. Jiang, Z. X. Xie, C. J. Lin, *Chem. Commun.* **2005**, 4181.

[19] W. Niu, S. Zheng, D. Wang, X. Liu, H. Li, S. Han, J. Chen, Z. Tang, G. Xu, *J. Am. Chem. Soc.* **2009**, *131*, 697.

[20] G. H. Jeong, M. Kim, Y. W. Lee, W. Choi, W. T. Oh, Q. H. Park, S. W. Han, *J. Am. Chem. Soc.* **2009**, *131*, 1672.

[21] R. Narayanan, M. A. El-Sayed, *Nano Lett.* **2004**, *4*, 1343.

[22] N. Tian, Z. Zhou, S. Sun, Y. Ding, Z. L. Wang, *Science* **2007**, *316*, 732.

[23] J. Xu, S. Li, J. Weng, X. Wang, Z. Zhou, K. Yang, M. Liu, X. Chen, Q. Cui, M. Cao, Q. Zhang, *Adv. Funct. Mater.* **2008**, *18*, 277.

[24] M. Zhou, S. Chen, S. Zhao, *J. Phys. Chem. B* **2006**, *110*, 4510.

[25] K. Kwon, K. Y. Lee, Y. W. Lee, M. Kim, J. Heo, S. J. Ahn, S. W. Han, *J. Phys. Chem. C* **2007**, *111*, 1161.

[26] C. Zhang, J. Zhang, B. Han, Y. Zhao, W. Li, *Green Chem.* **2008**, *10*, 1094.

[27] T. K. Sau, C. J. Murphy, *J. Am. Chem. Soc.* **2004**, *126*, 8648.

[28] L. Kuai, B. Geng, S. Wang, Y. Zhao, Y. Luo, H. Jiang, *Chem. Eur. J.* **2011**, *17*, 3482.

[29] P. T. Anastas, J. C. Warner, *Green Chemistry: Theory and Practice*, Oxford University Press, New York, **1998**.

[30] L. D. Marks, *Rep. Prog. Phys.* **1994**, *57*, 603.

[31] S. Ino, *J. Phys. Soc. Jpn.* **1966**, *21*, 346.

[32] Z. R. Tian, J. A. Voigt, J. Liu, B. Mckenzie, M. J. Mcdermott, *J. Am. Chem. Soc.* **2002**, *124*, 12954.

[33] T. Zhang, W. Dong, M. Keeter-Brewer, S. Konar, R. N. Njabon, Z. R. Tian, *J. Am. Chem. Soc.* **2006**, *128*, 10960.

[34] a) S. Yang, L. Gao, *J. Am. Chem. Soc.* **2006**, *128*, 9330.

[35] G. Falini, S. Albeck, S. Weiner, L. Addadi, *Science* **1996**, *271*, 67

[36] A. M. Belcher, X. H. Wu, R. J. Christensen, P. K. Hansma, G. D. Stucky, D. E. Morse, *Nature* **1996**, *381*, 56.

[37] S. Panigrahi, S. Basu, S. Praharaj, S. Pande, S. Jana, A. Pal, S. K. Ghosh, T. Pal, *J. Phys. Chem. C* **2007**, *111*, 4596.

[38] T. K. Sau, A. Pal, T. Pal, *J. Phys. Chem. B* **2001**, *105*, 9266.

[39] K. Esumi, K. Miyamoto, T. Yoshimura, *J. Colloid Interface Sci.* **2002**, *254*, 402.

[40] K. Hayakawa, T. Yoshimura, K. Esumi, *Langmuir* **2003**, *19*, 5517.

[41] J. Lee, J. C. Park, H. Song, *Adv. Mater.* **2008**, *20*, 1523.

[42] J. Turkevich, P. C. Stevenson, J. Hillier, *Discuss. Faraday Soc.* **1951**, *11*, 55.

[43] M. H. Rashid, T. K. Mandal, *Adv. Funct. Mater.* **2008**, *18*, 2261.

[44] G. A. Somorjai, *Introduction to Surface Chemistry and Catalysis*, Wiley, New York, **1994**.

[45] B. J. Hornstein, J. D. Aiken, III., R. G. Finke, *Inorg. Chem.* **2002**, *41*, 1625.

[46] M. Biswas, E. Dinda, M. H. Rashid, T. K. Mandal, *J. Colloid Interface Sci.* **2012**, *368*, 77.